

were made (Jonsson et al. measured at pH 8.9; we measured at 8.5).

The value of  $pK_{enz} = 7.6 \pm 0.6$  that we have estimated is consistent with the possibility that His-64 in the active-site cleft, which has been determined by NMR to have a  $pK_a$  near 7,<sup>19</sup> is the proton acceptor on the enzyme. In this case, His-64 could act as a proton shuttle to the activity-controlling group itself, for which there is evidence from isotope effect studies.<sup>15,20</sup> The data of Figure 3 considered alone are also consistent with proton transfer directly between the buffers and the activity-controlling group of  $pK_a$  near 7.

The data in Figure 3 appear to be in a transition region of the Brønsted plot, with values of  $k_4$  at pH near 9 approaching a plateau. The estimated limiting value of  $k_4$  from Figure 3 of  $(1.1 \pm 0.9) \times 10^9 \text{ M}^{-1} \text{ s}^{-1}$  can be compared with proton-transfer reactions between small molecules for which imidazole acts as a proton acceptor. In such a case, the diffusion-controlled value is approximated by the rate constant of  $1.2 \times 10^9 \text{ M}^{-1} \text{ s}^{-1}$  for proton transfer from acetic acid ( $pK_a = 4.8$ ) to imidazole.<sup>21</sup> In the reverse direction, the diffusion-controlled value is approximated by the rate constant of  $2 \times 10^{10} \text{ M}^{-1} \text{ s}^{-1}$  for proton transfer from imidazole to carbonate ( $pK_a = 10.3$ ).<sup>21</sup> This interesting comparison demonstrates that the diffusion-controlled limit in a proton-transfer

reaction involving buffer and the enzyme carbonic anhydrase is at least within a factor of 20 of the value for a small-molecule counterpart. This result is not likely to be influenced by limitations of the changing pH indicator method; the rate constant for combination of, for example, the indicator *p*-nitrophenol with  $\text{H}^+$  is in excess of  $10^{10} \text{ M}^{-1} \text{ s}^{-1}$ .<sup>22</sup>

It is our conclusion that, at least for low concentrations (<12 mM) of buffers, the rate-limiting proton transfer between human carbonic anhydrase II and external buffer is dependent on the  $pK$  difference between donor and acceptor species in a manner consistent with proton transfer between small molecules. The rate constant for the proton transfer follows a Brønsted curve that reaches a plateau at a value,  $1 \times 10^9 \text{ M}^{-1} \text{ s}^{-1}$ , very close to that found for proton transfer between small molecules. The transition region of the Brønsted plot indicates that the donor group on the enzyme has a  $pK_a = 7.6 \pm 0.6$ , which is consistent with proton transfer directly between the active site and buffer or between a proton shuttle group on the enzyme of  $pK_a$  near 7 and buffer.

**Acknowledgment.** We thank Professor Sven Lindskog and Dr. K. S. Venkatasubban for their very helpful comments. This work was supported by a grant from the National Institutes of Health (GM 25154).

**Registry No.**  $\text{CO}_2$ , 124-38-9; Mes, 4432-31-9; Hepes, 7365-45-9; Ted, 280-57-9; Ches, 103-47-9; 3,5-lutidine, 591-22-0; 3,4-lutidine, 583-58-4; 2,4-lutidine, 108-47-4; 1-methylimidazole, 616-47-7; triethanolamine, 102-71-6; 4-methylimidazole, 822-36-6; 1,2-dimethylimidazole, 1739-84-0; carbonic anhydrase II, 9001-03-0.

(19) Campbell, I. D.; Lindskog, S.; White, A. I. *J. Mol. Biol.* **1975**, *98*, 597-614.

(20) Venkatasubban, K. S.; Silverman, D. N. *Biochemistry* **1980**, *19*, 4984-4989.

(21) Eigen, M.; Hammes, G. G. *Adv. Enzymol. Relat. Subj. Biochem.* **1964**, *25*, 1-38.

(22) Eigen, M.; Kustin, K. *J. Am. Chem. Soc.* **1960**, *82*, 5952-5953.

## Interactions between Bilirubin and Albumins Using Picosecond Fluorescence and Circularly Polarized Luminescence Spectroscopy

Chieu D. Tran\* and Godfrey S. Beddard†

Contribution from the Davy Faraday Research Laboratory of the Royal Institution, 21 Albermarle Street, London W1X 4BS, U.K. Received July 9, 1981

**Abstract:** Circular dichroism, circularly polarized luminescence, and time-resolved picosecond fluorescence spectroscopy have been used to study the interaction between bilirubin (BR), human serum albumin (HSA), bovine serum albumin (BSA) at several pH's, albumin/BR ratios, and salt concentrations. The BR single excited state when bound to albumin is in a right-handed helical conformation, similar to that of the ground state except near pH 4.1, where the ground state takes up a left-handed conformation. Solutions of bilirubin exhibit biexponential fluorescence decays, with the major decay ( $\sim 30$  ps) being attributable to BR while the minor decay ( $\sim 1$  ns) is due to photoproducts of BR, possibly *Z,E*, *E,Z*, and *E,E* geometric isomers. The maximum rate of photoisomerization from BR is calculated as  $5 \times 10^{10} \text{ s}^{-1}$  and that of the isomers is  $5 \times 10^8$  to  $10^9 \text{ s}^{-1}$ . When bound to HSA, bilirubin and its photoproduct appear to attach themselves to different types of binding sites since BR excited singlet decay times are unaffected by salt or pH whereas the photoproducts decay times are sensitive to these factors.

About 20% of newborn infants develop jaundice during their first 3-4 days because of the inefficiency of their hepatic function and the short lifetime of their red blood cells.<sup>1</sup> Bilirubin (BR),<sup>2</sup> the catabolic product of blood heme, builds up in the blood plasma, enters fatty tissue, and hence causes neonatal jaundice.<sup>1</sup> Bilirubin binds strongly to serum albumin, and this binding lowers the level of free BR in blood plasma.<sup>3</sup> Because of the small amount of albumin in newborn infants, it is necessary to perform phototherapy in order to lower BR levels of those suffering from extreme

jaundice, thus preventing the damaging effects of BR on the brain (kernicterus) and other organs.<sup>1,4</sup>

The binding of bilirubin to albumins has been studied extensively by NMR,<sup>5</sup> visible absorption,<sup>6</sup> CD,<sup>6,7</sup> ORD,<sup>8</sup> and fluorescence

\* Address correspondence to Department of Chemistry, Clarkson College of Technology, Potsdam, NY 13676.

† Present address: Department of Chemistry, University of Manchester, Manchester M13 9PL, U.K.

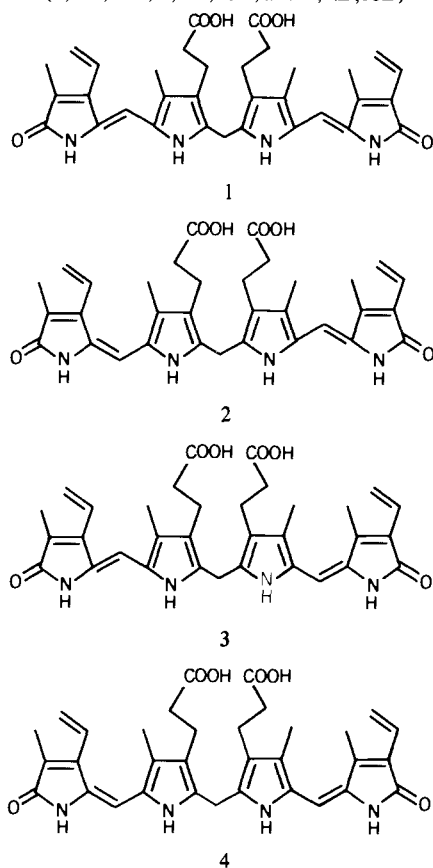
(1) (a) Karp, W. B. *Pediatrics* **1979**, *64*, 361-368. (b) Brodersen, R. *CRC Crit. Rev. Clin. Lab. Sci.* **1980**, *11*, 305-399.

(2) Abbreviations: BR, (4Z,15Z) bilirubin IX $\alpha$ , PBR, photobilirubin or *E,Z*, *Z,E*, or *E,E* isomers of BR; HSA, human serum albumin; BSA, bovine serum albumin; HBR, 3,4-diethyl-5-(3,4-diethyl-5-methylpyrrol-2-yl methylidene)-3-pyrrolin-2-one.

(3) Chen, R. F. *Arch. Biochem. Biophys.* **1974**, *160*, 106-112.

(4) McDonagh, A. F.; Palma, L. A.; Lightner, D. A. *Science (Washington, D.C.)* **1980**, *208*, 145-151.

Scheme I. Structure of Bilirubin (1, 4Z,15Z) and Its Photoproducts (2, 4E,15Z; 3, 4Z,15E; and 4, 4E,15E)



spectroscopy,<sup>6,7</sup> while the occurrence of multiple binding sites and the location of BR within human serum albumin and bovine serum albumin have been inferred from CD and fluorescence studies.<sup>3,9,10</sup> There is, however, comparatively little photophysical information on BR excited states, or excited state conformations, when it is bound to albumins, although this information is of particular importance because of its intimate connection with the phototherapy of neonatal jaundice.<sup>11</sup> Lightner et al. have shown that BR undergoes configurational photoisomerization about the meso double bonds to the so-called photobilirubin, which is probably a mixture of *Z,E*, *E,Z*, and *E,E* configurational isomers (see Scheme I), but the precise mechanism for this process is still not fully understood.<sup>11-13</sup> Photooxidation<sup>14</sup> and degradation<sup>15</sup> also occur, but with quantum yields significantly lower ( $\sim 0.1$ ) than those of photoisomerization.<sup>4,11-13</sup>

The photophysical properties of BR are governed by nonradiative pathways out of the excited singlet state ( $S_1^*$ ) because of its low fluorescence quantum yield ( $\sim 10^{-4}$ )<sup>16</sup> and short singlet lifetime (20–70 ps).<sup>18,19</sup> On binding to albumin, the fluorescence

yield of BR is still small but increases to  $2 \times 10^{-3}$ , while the excited singlet decay is still in the range 30–70 ps.<sup>3,19</sup>

The excited-state conformation of BR can be obtained by studying the circular polarization of the BR fluorescence since BR becomes optically active upon binding to albumins.<sup>6-8,10</sup> We have studied this binding using circularly polarized luminescence (CPL). A picosecond mode-locked argon ion laser with a time-correlated single-photon-counting fluorescence detection system is also used to study the excited-singlet-state lifetimes of BR bound to HSA and BSA under a variety of conditions including pH, album to BR ratios, and electrolyte concentrations.

### Experimental Procedures

**Materials.** Bilirubin IX $\alpha$  (Sigma) was used as received since it showed a single spot on polyamide thin-layer chromatography plates (Polyamid 10F 254 Merck) with methanol/water (3:1, v/v)<sup>20</sup> and its extinction coefficient in chloroform at 543 nm was  $6.0 \times 10^4 \text{ M}^{-1} \text{ cm}^{-1}$ , in agreement with the accepted value for the pure pigment.<sup>3</sup> Moreover, the results obtained from this bilirubin are identical with those of purified samples of bilirubin IX $\alpha$ , which were generously supplied by Professor D. Lightner. Essentially fatty acid free HSA (Sigma lot 70F9310) and BSA (Sigma lot 10F9370) were used as received, and details of sample preparation are given in ref 19, and 21.

**Instrumentation.** Absorption spectra were recorded on a Perkin Elmer 554 spectrometer; a Jasco J-40CS was used to measure CD spectra. For details of CPL instrumentation, see Barnett et al.<sup>22</sup> Absorption ( $g_{\text{abs}}$ ) and emission ( $g_{\text{em}}$ ) dissymmetry factors are defined as  $g_{\text{abs}} = (\text{OD}_L - \text{OD}_R)/\text{OD}$  and  $g_{\text{em}} = (I_L - I_R)/I$ , where  $(\text{OD}_L - \text{OD}_R)$  is the differential optical density for left and right circularly polarized light of a solution having an isotropic optical density OD ( $\text{OD} = \frac{1}{2}(\text{OD}_L + \text{OD}_R)$ ) and emitting a total isotropic fluorescence intensity  $I$  ( $I = \frac{1}{2}(I_L + I_R)$ ) and a differential circularly polarized luminescence ( $I_L - I_R$ ).

The 476-nm line of an argon ion laser (Coherent Radiation CR6) was mode locked and, after the pulse-to-pulse repetition rate was reduced to 50 kHz by a repetitively pulsed Pockels cell, was used to excite the fluorescence.<sup>19,23</sup> The laser power was reduced to  $< 10 \mu\text{W}/\text{cm}^2$  so that no unwanted photolysis of the BR occurred during the measurements.

The acoustooptic mode locker was driven by a radiofrequency source and amplifier. This combination has a frequency stability of better than 10 Hz, which is necessary to obtain good mode locking over periods of several days. The 476-nm pulse had a half-width of 90 ps as measured by a fast photodiode and a S6 sampling head. Furthermore, high pulse-to-pulse reproducibility in both amplitude and duration was observed by the almost complete lack of jitter and smooth trace on the sampling scope. Fluorescence was detected at  $90^\circ$  to vertical excitation through a polarizer at  $54.7^\circ$  and interference filters (8-nm band pass, 525, 555, and 575 nm) as described previously.<sup>19,23</sup>

The fluorescence decay times were obtained by the convolution of the measured instrument response (laser light scattered from dilute talc) with trial functions to fit to the experimentally measured fluorescence. Iterations to obtain a fit to the data were performed by nonlinear least-squares algorithm assuming that the fluorescence decayed either as a single exponential or as a sum of exponential terms, i.e.,  $I(t)$ , the fluorescence intensity at time  $t$ , was assumed to be of the form

$$I(t) = A(fe^{-t/\tau_1} + (1-f)e^{-t/\tau_2}) + B \quad (1)$$

where  $\tau_1$ , and  $\tau_2$  are the short and long decay lifetimes, respectively,  $f$  is the fraction of the component with decay  $\tau_1$ ,  $A$  is the total amplitude, and  $B$  is the background due to photomultiplier and other noise. A shift function was used to account for the changing wavelength response of the photomultiplier<sup>23</sup> and, also, the use of filters of different thickness in the light path. Precision of fit was estimated by the  $\chi^2$  parameter of 1.2 or better over the whole set of data points, and the residuals and covariance matrix were also inspected. The shorter measured decay times (20–30 psc) represent a realistic lower limit on lifetime measurements with this particular technique and are considerably shorter than those

(5) Kuenzle, C. C.; Weibel, M. H.; Pelloni, R. R.; Hemmerich, P. *Biochem. J.* **1973**, *133*, 364–368.

(6) Blauer, G.; Harmatz, D. *Biochim. Biophys. Acta* **1972**, *278*, 68–82.

(7) Blauer, G.; Wagniere, G. *J. Am. Chem. Soc.* **1975**, *97*, 1949–1954.

(8) Blauer, G.; King, T. E. *J. Biol. Chem.* **1970**, *245*, 372–381.

(9) Chen, R. F. In "Fluorescence Techniques in Cell Biology"; Thae, A., Sernetz, M., Eds.; Springer-Verlag: New York, 1974; pp 239–243.

(10) Beavan, G. H.; d'Albis, A.; Gratzer, W. B. *Eur. J. Biochem.* **1973**, *33*, 500–510.

(11) Lightner, D. A. *Photochem. Photobiol.* **1977**, *26*, 427–436.

(12) Lightner, D. A.; Wooldridge, T. A. *Biochem. Biophys. Res. Commun.* **1979**, *86*, 235–243.

(13) Lightner, D. A.; Wooldridge, T. A.; McDonagh, A. F. *Proc. Natl. Acad. Sci. U.S.A.* **1979**, *76*, 29–32.

(14) Lightner, D. A.; Cu, A. *Life Sci.* **1977**, *15*, 723–727.

(15) Bonnett, R. *Biochem. Soc. Trans.* **1976**, *4*, 222–226.

(16) Holzwarth, A. R.; Lehner, H.; Braslausky, S. E.; Schaffner, K. *Liebigs. Ann. Chem.* **1978**, 2000–2017.

(17) Tredwell, C. T.; Keary, C. *Chem. Phys.* **1979**, *43*, 307–316.

(18) Greene, B. I.; Lamola, A. A.; Shank, C. V. *Proc. Natl. Acad. Sci. U.S.A.* **1981**, *78*, 2008–2012.

(19) Tran, C. D.; Beddard, G. S. *Biochim. Biophys. Acta* **1981**, *678*, 497–504.

(20) Petryka, Z. J.; Watson, C. J. *J. Chromatogr.* **1968**, *37*, 76–82.

(21) Tran, C. D.; Drake, A. F. *Biochem. Biophys. Res. Commun.* **1981**, *101*, 76–82.

(22) Barnett, C. J.; A. F.; Mason, S. F. *Bull. Soc. Chim. Belg.* **1979**, *88*, 853–862.

(23) Robbins, R. J.; Fleming, G. R.; Beddard, G. S.; Robinson, G. W.; Thistlethwaite, P. J.; Woolfe, G. J. *J. Am. Chem. Soc.* **1980**, *102*, 6271–6279.

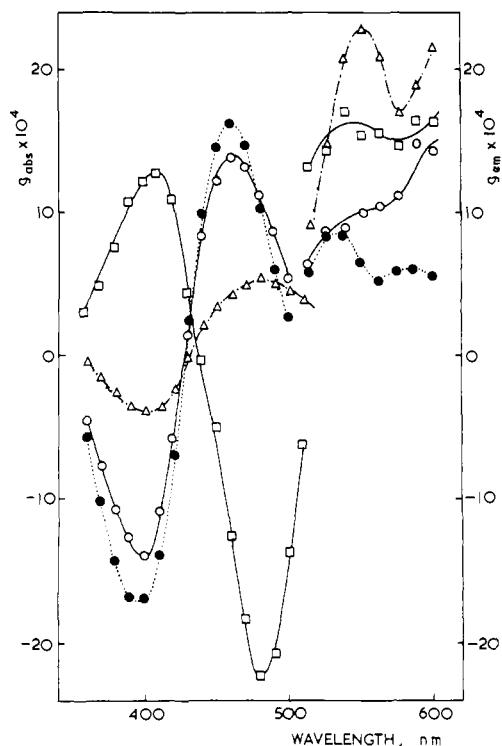


**Figure 1.** Absorption ( $g_{\text{abs}}$ ) and emission ( $g_{\text{em}}$ ) dissymmetry factors of  $5 \times 10^{-5}$  M BR bound to  $5 \times 10^{-5}$  M HSA in  $5 \times 10^{-3}$  M buffer at pH 4.1 ( $\square$ ), 4.8 ( $\Delta$ ), 7.4 ( $\circ$ ), and 9.0 ( $\bullet$ ).

previously assumed to be measurable. In analyses of such short decays, the nonlinear least-squares routines appear to require the presence of a longer component ( $\tau_2$ ) in order to converge well to parameter values that are largely independent of the starting values. An example of a fluorescence decay is shown in Figure 2, where the narrow line is the instrument response function (i.e., the laser pulse distorted by the photomultiplier, discriminator, and associated electronics), the points are the measured fluorescence decay, and the line through these points is the calculated best fit to the data for a two-exponential function with lifetimes of  $\tau_1 = 63$  ps and  $\tau_2 = 2020$  ps. Over a number of experiments, precision of  $\pm 15\%$  on the shorter decay times and  $\pm 10\%$  on the longer ones was achieved. We checked the accuracy of the values by comparison with short-fluorescence-lifetime dyes measured with a streak camera<sup>17</sup> having a 2-ps resolution. The short BR decay times ( $\tau_1$ ) are also close to those reported recently from picosecond absorption measurements.<sup>18</sup>

## Results

**CD and CPL Spectra of BR Bound to BSA.** CD spectra of  $5 \times 10^{-5}$  M BR and  $5 \times 10^{-5}$  M BSA in  $5 \times 10^{-3}$  M buffer at pH 4.0, 5.0, 7.4, and 9.0 (not shown) were qualitatively the same as those reported elsewhere.<sup>6,10</sup> Even though BR bound to BSA shows strong fluorescence ( $\lambda_{\text{max}}$  530 nm, excitation 460 nm), no circularly polarized luminescence was detected over a pH range from 4 to 9. Therefore, BR bound to the BSA was used to calibrate the base line for CPL.

**CD and CPL Spectra of BR Bound to HSA.** The chiroptical parameters ( $g_{\text{abs}}$  and  $g_{\text{em}}$ ) of  $5 \times 10^{-5}$  M BR and  $5 \times 10^{-5}$  M HSA in  $5 \times 10^{-3}$  M buffer at pH 4.1, 4.8, 7.4, and 9.0 are shown in Figure 1. The absorption dissymmetry factors agree qualitatively with those derived from the reports of Blauer<sup>6</sup> and Beavan<sup>10</sup> and show a general decrease from pH 9 to 4.8 and a sign reversal at pH 4.1. The sine-wave-like nature of the CD results from a particular dihedral angle between the two dipyrromethene moieties of the bound BR while the sign change at pH 4.1 can be considered to be connected with the change in albumin structure.<sup>10</sup> The emission dissymmetry ( $g_{\text{em}}$ ) of BR in HSA changes rapidly over wavelengths from 500 to 600 nm, indicating either that the emitting species, due to environmental perturbations, have different energy levels<sup>24</sup> or that there is more than one chemically different emitting species<sup>24</sup> (Figure 1). At pH 4.8, 7.4, and 9.0, the  $g_{\text{em}}$  are almost

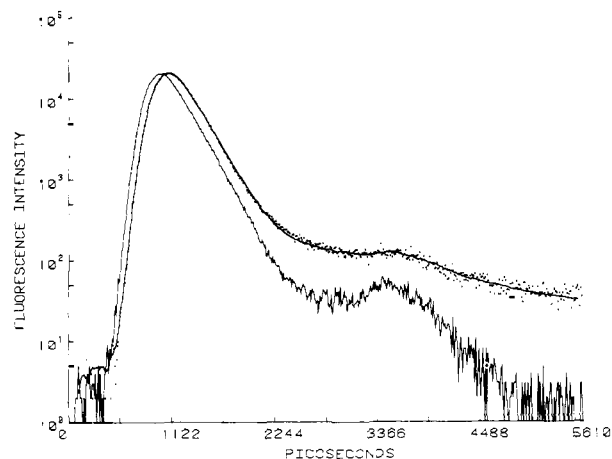


**Figure 2.** Fluorescence decay of  $5 \times 10^{-5}$  M BR bound to  $5 \times 10^{-5}$  M BSA in  $5 \times 10^{-3}$  M borate buffer at pH 9.0 at 11 ps/channel. The semilog plot shows the instrument response function as a narrow solid line, the fluorescence as dots, and the calculated decay curve as a smooth solid line through the dots. A two-exponential fit to the data gives  $\tau_1 = 63$  ps and  $\tau_2 = 2020$  ps.

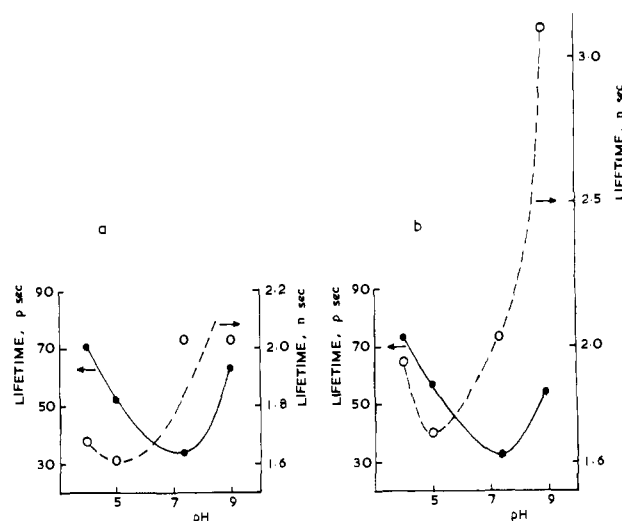


**Figure 3.** Fluorescence lifetimes of  $5 \times 10^{-5}$  M BR bound to  $5 \times 10^{-5}$  M BSA in  $5 \times 10^{-3}$  M buffer at different pH.  $\tau_1$  ( $\bullet$ ) is the short decay time and  $\tau_2$  ( $\circ$ ) the long decay time fluorescence at (a) 525 nm and (b) 575 nm.

the mirror images of the  $g_{\text{abs}}$  from 500 to 530 nm, implying that the species emitting at this wavelength has the same conformation as the ground state. However, the species emitting at wavelengths longer than 530 nm has a different conformation.

The pH dependence of the magnitude of  $g_{\text{em}}$  is the inverse of that of  $g_{\text{abs}}$ , which decreases as the pH changes from 9.0 to 4.8 (Figure 1). At pH 4.1, there is an inversion between  $g_{\text{em}}$  and  $g_{\text{abs}}$ , and BR takes up a left-handed helical conformation in the ground state<sup>7,21</sup> but transforms to a right-handed conformation in the excited state.<sup>21,24</sup> To the best of our knowledge, this is the first observation of a complete inversion of configuration between the ground and excited states.

**Fluorescence Lifetimes of BR Bound to BSA.** The presence of more than one emitting species in the albumin-BR samples has been observed also by fluorescence-lifetime measurements (Figure 2). Fluorescence lifetimes as a function of pH are shown for BSA in Figure 3a, (emission wavelength 525 nm) and Figure 3b (emission wavelength 575 nm).

The excited singlet state of BR decayed biexponentially; almost 99% of the initial fluorescence intensity had a lifetime in the range 30–75 ps (filled circles, Figure 3) while the remaining 1% had a lifetime from 1.6 to 2.2 ns (open circles). The fraction of the shorter lifetime component in the total decay decreased and that of the longer one increased as the detection wavelength was

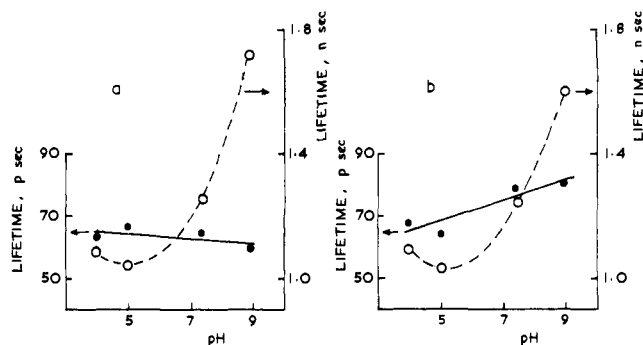


**Figure 4.** Fluorescence lifetimes of  $5 \times 10^{-5}$  M BR bound to  $5 \times 10^{-5}$  M HSA in  $5 \times 10^{-5}$  M buffer at different pH. Conditions as in Figure 3.

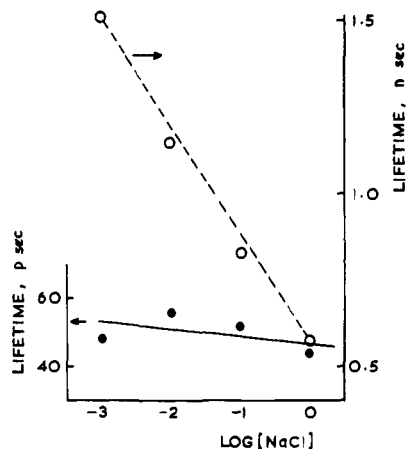


**Figure 5.** Fluorescence lifetimes of  $5 \times 10^{-5}$  M BR bound to  $5 \times 10^{-5}$  M HSA in  $5 \times 10^{-3}$  M phosphate buffer at pH 7.4 at different NaCl concentrations.

changed from 525 (Figure 3a) to 575 nm (Figure 3b). The effect of pH on the fluorescence lifetimes is shown in Figure 3 a and b, where the detection wavelengths were 525 and 575 nm, respectively. The shorter lifetime decreased as the pH was increased from 4.0 to 5.0, reaching a minimum (33 ps) at pH 7.4 (Figure 3a). The longer lifetime component ( $\tau_2$ ) reaches a minimum at pH 5 but increases rapidly with pH to 3.1 ns at pH 9 at 575 nm (Figure 3b). We shall show later that the short lifetime ( $\tau_1$ ) is associated with BR and the longer lifetime ( $\tau_2$ ) with the photoisomers (PBR) in membrane solution<sup>19</sup> and protein.

**Fluorescence Lifetimes of BR Bound to HSA.** As in the case of BSA, the fluorescence of HSA-bound BR decayed biexponentially; almost 99% of the initial intensity was associated with the shorter lifetime (Figure 2). The fraction of the longer decaying component increased between 525 and 575 nm. The relationship between fluorescence lifetime of bound HSA at different pH values is shown in Figure 4a (fluorescence detected at 525 nm) and b (detected at 575 nm). Interestingly, the pH dependence of  $\tau_1$  (short decay) and  $\tau_2$  are different for HSA than for BSA since  $\tau_2$  has a minimum value at pH 5 and maximum at pH 9. In HSA, the shorter component ( $\tau_1$ ), however, remains constant over the pH range 4–9, while in BSA,  $\tau_1$  shows a minimum at pH 7.

Figure 5 shows the effect of sodium chloride concentration upon the fluorescence decays  $\tau_1$  and  $\tau_2$  measured at 575 nm with equimolar amounts of HSA and BR at pH 7.4. As can be seen, the major decay ( $\tau_1$ , filled circles) is not affected by NaCl concentration within experimental error, but the longer decay ( $\tau_2$ , open circles) decreased with increasing NaCl concentration. The relationship between  $\tau_1$  and  $\tau_2$  and HSA/BR ratio is shown in Figure 6, a (at 525 nm) and b (at 575 nm). At low ratios (<1), the fluorescence decays do not fit well with a two-exponential analysis ( $\chi^2 \sim 2.0$ ), but, surprisingly, the fitting became worse when decays were fitted to three-exponential terms. These observations can be explained by the supposition that there are more

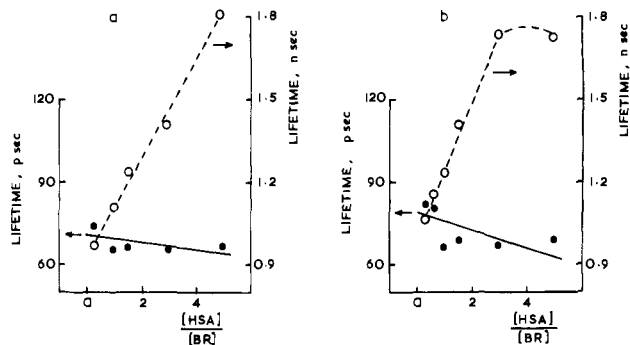


**Figure 6.** Fluorescence lifetimes of  $5 \times 10^{-5}$  M BR in  $5 \times 10^{-3}$  M phosphate buffer (pH 7.4) at different HSA concentrations. Conditions as in Figure 4.

than three components in the decay under these conditions. The short decay ( $\tau_1$ ) dominates the decay so that the remaining 1% at the onset of the decay is of too little intensity to fit properly to more than one term. The best double-exponential-fitting lifetimes vs. HSA/BR ratios are shown in Figure 6, a and b. From these figures, it is seen that increasing the HSA/BR ratios from 3 to 5 increases the long decay ( $\tau_2$ , open circles) but, within experimental error, does not affect  $\tau_1$  (filled circles).

## Discussion

**Conformation of BR Bound to Albumin.** The very large dissymmetry factors ( $g_{\text{abs}} > 10^{-3}$ ) observed for BR bound to BSA and HSA suggest that the BR is rigidly immobilized on the albumins in a configuration that possesses an inherent helical shape, rather than in a symmetrical arrangement perturbed only by dissymmetry in the binding site as in the case of DNA-induced optical activity of acridine dyes.<sup>10,24</sup> X-ray crystallography studies<sup>25,26</sup> have shown that BR achieves dissymmetric conformation by intramolecular hydrogen bonds between -COOH and -NH groups on the pyrrole. Because of this dissymmetric conformation, the electronic-transition dipole moments of the dipyrromethene chromophores of BR becomes juxtaposed, and electric dipole-dipole coupling is responsible for the optical activity of albumin-bound BR.<sup>67</sup> From the calculated dipole and rotatory strengths, Blauer and Wagniere<sup>7</sup> conclude that BR bound to HSA adopts a right-handed conformation at pH 4.8, 7.4, and 9.0 but takes up a left-handed helical conformation at pH 4.1.<sup>67</sup> In this region two forms, of HSA are observed by electrophoresis experiments, the normal N form, which alone exists at about pH 4.5, while a new form, which in electrophoresis moves ahead, is called the F form. At low pH, protonation of the albumin is probably responsible for the transition from N to F forms.<sup>1b,27</sup> The change in conformation of BR at pH 4.1 is thus associated with the change to the F form of the protein.<sup>1b,21</sup>

The change in the size and shape of the CD signal with pH possibly reflects the different hydrogen bonding either of the BR with itself, at different pH, as the two halves of the BR fold back toward one another to form part of a helix turn<sup>11,29</sup> or of the BR to some of the many carboxyl groups in the protein; this bonding can also change with pH. At pH 4.8, the BR is a mixture of two types of conformations, the conformation at high pH and that at low pH, so that the overall  $g_{\text{abs}}$  is small since this is the sum of left- and right-handed forms of BR (Figure 1). Presumably, there is a pH between pH 4.1 and 4.8 where  $g_{\text{abs}}$  is essentially zero.<sup>1b</sup> As the pH increases to 9,  $g_{\text{abs}}$  becomes larger since the BR binding to the protein becomes stronger.<sup>1b</sup>

(25) Bonnett, R.; Davies, J. E.; Hursthouse, M. B. *Nature (London)* **1976**, *262*, 326.

(26) Bonnett, R.; Davies, J. E.; Hursthouse, M. B.; Sheldrick, G. M. *Proc. R. Soc. London, Ser. B* **1978**, *202*, 249.

(27) Foster, J. F. In "The Plasma Protein"; Putham, F. W., Ed; Academic Press: New York, 1960; pp 179-239.

(28) Hansen, P. E.; Thiesch, H.; Brodersen, R. *Acta Chem. Scand., Ser. B* **1979**, *B33*, 281-293.

(29) Lee, J. J.; Gillespie, G. D. *Photochem. Photobiol.* **1981**, *33*, 757-760.

Scheme II



We have previously suggested that (at pH >4.1) the species emitting below 530 nm are of the *Z,Z* isomeric form of BR while, above 530 nm, photobilirubins (*Z,E*, *E,Z*, *E,E* photoisomers) contribute to the fluorescence<sup>19,21</sup> (Scheme I). Up to 530 nm,  $g_{em}$  mirrors  $g_{abs}$ , as it should for a single species, but from 530 to 600 nm, there is sufficient difference between these two parameters to confirm the suggestion of two or more emitting species (i.e., BR and its photoisomers) contributing to the total fluorescence (Figure 1).

In the ideal case where there is neither change of geometry in the excited state compared to the ground state nor change in the electronic-transition dipole-moment direction between emission and absorption then for a particular transition,  $g_{abs} = g_{em}$ .<sup>24</sup> The sign and magnitude of the lowest energy absorption CD band can be correlated with the molecular chirality of BR bound to HSA, or, more particularly, with the resultant dihedral angle between the two dipyrromethene residues.<sup>6,7</sup> Therefore, any differences in  $g_{em}$ , specifically with respect to  $g_{abs}$ , can indicate also changes in this dihedral angle. Thus the pH dependency of  $g_{em}$  may result from a change in geometry upon excitation. With reference to the work of Blauer and Wagniere,<sup>6,7</sup> it is concluded that the resultant dihedral angle between the dipyrromethene moieties of BR bound to HSA is much greater in the excited state than in the ground state at pH 4.8, 7.4, and 9.0; in other words, upon excitation, bound BR prefers to adopt a more extended structure. At pH 4.1, BR bound to HSA takes up a left-handed helical conformation in the ground state but transforms into a right-handed conformation in the excited state (square symbols, Figure 1).

The change from left- to right-handed helices upon excitation at pH 4.1 needs explanation because of the short excited-state lifetime. In view of the experimental observations, it seems that the stability of the interactions of BR with the protein, which hold it in the left form, may be only marginally greater than those needed for the right-handed helical form. This suggestion is not, however, unreasonable since the energy barrier for a complete configurational inversion of BR is almost negligible as calculated by Manitto et al.<sup>30</sup> The only requirement for this process is 38 kJ/mol, which is required to rupture the hydrogen bonds.<sup>30</sup> We propose the following tentative suggestion for the change of left- to right-handed forms. At the instant the BR excited state is formed, it has the ground state geometry; the charge redistribution in the molecule upon excitation initiates geometry changes experienced as the molecule decays. Before these changes can occur, the hydrogen bonds formed with the carbonyl groups on either side of the molecule, or with the protein, must break. However, the change from left- to right-handed species need not necessarily involve a large geometry change and can consequently be rapid. Let us suppose that the BR is represented by a structure A-CH<sub>2</sub>-A<sup>1</sup> (since the ring substituents are different) folded into a "V" with -CH<sub>2</sub>- at the apex, in one form the A<sup>1</sup> moiety will be above the A, (Scheme IIA). The C-CH<sub>2</sub>-C bonds can undergo a "bicycle pedal" motion, still retaining a V shape but now with A<sup>1</sup> below A as in Scheme IB, to produce the other helix. This involves only a small volume change and hence could occur rapidly. It is then possible that in BR the change from left to right helix geometry can occur in a time significantly shorter than the excited state lifetime that is essential for the circularly polarized luminescence to be observable. As may be seen in Figure 1, the dissymmetry factor  $g_{em}$  has, between 600 and 530 nm and at pH

Table I. Excited Singlet Decay Times of BR

	$\tau_1$ , <sup>a</sup> ps	$\tau_2$ , ps	$f$
BR, BSA	63	2020	99.8
BR, HSA	64	1100	98.6
BR, <sup>b</sup> pyridine	49	2530	99.9
BR, <sup>b</sup> CCl <sub>4</sub>	14	1200	99.9
HBR, <sup>b</sup> pyridine	78	2860	94

<sup>a</sup>  $\tau_1$ ,  $\tau_2$ , and  $f$  defined in eq 1, excitation 476 nm, detection 550 nm. <sup>b</sup> From ref 19.

4.1 and 9.0, the same values, which are smaller relative to those values at pH 4.8. Since the emission dissymmetry factor  $g_{em}$  has the same sign as each pH, the large  $g_{em}$  at pH 4.8 is due to the addition of  $g_{em}$ 's from both types of structures present at this pH at a result of a combination of left- and right-handed ground-state conformers.

At wavelengths longer than 530 nm the fluorescence is complicated by emission from isomeric photobilirubin species. The direction of the transition electric dipole moment in these geometric (*E,Z*, *Z,E*, *E,E*) isomers will necessarily be different from that in the parent ground-state *Z,Z* isomer, and the observed dissymmetry factors will be accordingly different.<sup>7</sup> All that can be reasonably suggested at this stage is that the variation of  $g_{em}$  with wavelength confirms the existence of these isomers in the excited state and that they appear to adopt an excited-state conformation that is associated with a positive dissymmetry factor. The pH dependence of  $g_{em}$  in this wavelength region can be interpreted as involving changes in the molecular conformations, although a change in the relative amounts of various geometric isomers may also be important in this case.<sup>19,21</sup>

While the CPL results are very useful in elucidating excited-state conformation of the fluorophore, they are, however, not very sensitive in providing information about binding sites or about the location of a fluorophore. This information can be provided by fluorescence measurements, which are discussed after we have described the photophysics of bilirubin.

**Bilirubin Photophysics.** The natural radiative lifetime ( $k_f^{-1}$ ) of BR in solution is  $\sim 20$  ns,<sup>18,19</sup> although the measured decay time is  $\sim 10^{-3}$  of this value, see Table I; the fluorescence yield is similarly small,  $\sim 5 \times 10^{-4}$ .<sup>16</sup> These observations indicate that the nonradiative pathways depleting the excited singlet state ( $S_1^*$ ) dominate the decay process. At low temperatures (77 K) where isomerization is almost frozen out, the fluorescence yield rises to  $\sim 0.5$ ,<sup>18</sup> and as no triplets are formed,<sup>31</sup> internal conversion to  $S_0$  at a rate  $k_{IC}$  must deplete  $S_1^*$ , with the rate constant  $k_{IC}$  comparable to  $k_f$ , i.e.,  $\sim 5 \times 10^7$  s<sup>-1</sup>.

At room temperature the rapid excited-singlet decay will be governed by the nonradiative pathways, one of which leads to photoisomerization<sup>4,18</sup> about the *4Z* or *15Z* bonds to give the *4E* or *15E* isomers or both (Scheme I). The reason for these fast processes occurring in BR and not in porphyrins, from which BR is formed and whose lifetimes are of the order of a few nanoseconds,<sup>32</sup> may be seen from BR structure since it has been proposed that, in common with many similar types of molecules, the excited singlet state of this molecule may twist about its exocyclic double bonds (in the ground state, *4Z* = *15Z*), eventually leading to photoisomerization.<sup>18</sup> This twisting will be impeded by viscous drag of the solvent on the molecule and also by any intramolecular hydrogen bond but enhanced by electronic effects as the molecule attempts to reach its excited-state equilibrium geometry.<sup>33</sup>

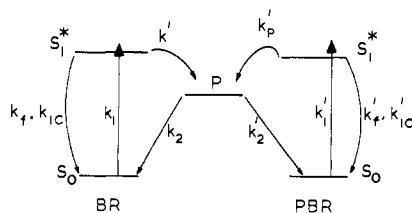
Free bilirubin fluorescence is known to increase with increasing solvent polarity and dielectric constant.<sup>19,29</sup> In CHCl<sub>3</sub> when the BR is intramolecularly hydrogen bonded,<sup>11</sup> the excited singlet decay ( $\tau_1$ ) is 14 ps. As the solvent polarity is increased, these hydrogen bonds are disrupted, resulting in an increased singlet lifetime and yield; i.e., in pyridine,  $\tau_1 = 49$  ps. Also in a dipyrrole,

(31) Sloper, R. W.; Truscott, T. G. *Photochem. Photobiol.* **1980**, *31*, 445-450.

(32) Harriman, A. *J. Chem. Soc., Faraday Trans. 1* **1980**, *76*, 1978-1985.

(33) Rice, S. A. In "Excited States"; Lim, E. C., Ed.; Academic Press: New York 1975; pp 111-320.

Scheme III



which is a model for half-bilirubin (HBR)<sup>2</sup> in which isomerization but no intramolecular hydrogen bonding can occur,<sup>19</sup> the decay times are about twice those of BR;  $\tau_1$  in pyridine = 78 ps (Table I).

The effect of intramolecular hydrogen bonds could be twofold: firstly, in resisting the photoisomerization as it presents an energy barrier of at least 30 kJ/mol to break the hydrogen bonds,<sup>30</sup> and secondly, the formation of the hydrogen bonds could distort the molecule about the 4Z or 15Z double bonds and lead to a reduction in the excited singlet decay lifetime as indicated above. This distortion (twisting) of the double bonds is similar to that which is believed to occur in the conjugated cyanines, which also have extremely short decay times.<sup>17,34</sup> This twisting process should lead to extra internal conversion to  $S_0$  rather than isomerization, but it is possible that the distortion of these double bonds offsets to some extent the stabilization provided by hydrogen bonding on the reaction pathway that leads to isomerization.

Picosecond experiments on the excited singlet of *trans*-stilbene lead to an excited-state lifetime governed by isomerization at a rate of 70 ps<sup>-1</sup>,<sup>35,36</sup> the lifetime of half-bilirubin (HBR) in pyridine is of this order ( $\tau_1 = 80$  ps)<sup>19</sup> and may represent the rate of photoisomerization about the Z-E bonds in BR; i.e., isomerization rate = (80 ps)<sup>-1</sup> =  $1.25 \times 10^{10}$  s<sup>-1</sup>. As the BR lifetime is approximately 20 ps in solution,<sup>19</sup> we propose that to account for the discrepancy in decay times between BR and HBR, the rate of the internal conversion in BR due to distortion of the double bonds by hydrogen bonding is approximately 20–80 ps<sup>-1</sup> =  $3.75 \times 10^{10}$  s<sup>-1</sup>. (Intramolecular hydrogen bonds in BR should make its isomerization slower than that in HBR.)

The pathway to isomerization could follow a scheme similar to that proposed for other compounds containing exocyclic double bonds such as the stilbenes,<sup>35,36</sup> where there is a small activation energy on a pathway leading from  $S_1^*$  toward an intermediate "twisted singlet state" (P) (Scheme III) of lower energy than  $S_1^*$ . This same twisted state can also be reached from the excited singlet state of the photoisomer PBR. There are pathways leading to the destruction of the twisted singlet state: viz., either the ground state corresponding to the initially excited singlet ( $S_0$  of BR, scheme III) or the ground state of the other isomers ( $S_0$  to PBR). Such a stilbene-type model has recently been proposed for BR,<sup>18</sup> where the rates of decay ( $k_2$ ,  $k_2'$ ) of the twisted intermediate state were proposed to be much faster than the rate constant  $k_p$  of entering this state over the potential barrier. The rate constant  $k_p$  is then the rate-limiting step in the photoisomerization. This potential barrier must, however, be small since the rate for this process is high ( $1.25 \times 10^{10}$  s<sup>-1</sup>). When bound to albumin, the ability of BR to twist from the excited singlet state must be slightly more restricted since the singlet lifetime is longer (66 ps, Table I) than, that in a solvent where intramolecular hydrogen bonds are possible (14 ps in CHCl<sub>3</sub>, Table I). In each of the samples studied, a long component of small intensity, ~1% at the onset of the decay, was observed. The intensity of this component increased as measurements were taken toward longer wavelengths (525 → 575 nm) in both albumins and solutions. We have pre-

viously shown<sup>19</sup> that the emission decaying with the longer lifetime ( $\tau_2$ ) and also present at longer wavelengths is due to the fluorescence from the excited singlet state of one or more of the photoisomer.<sup>19</sup>

Picosecond experiments on the photoisomers of BR alone proved impossible since BR is always present in large excess. Greene et al.<sup>18</sup> have suggested on the basis of quantum yield measurements that the singlet decay time for the photoisomer should be ~0.1 ps. From direct measurements, we have shown,<sup>19</sup> however, that this decay time is 1–2 ns. The rate constants for fluorescence and internal conversion ( $k_f'$ ,  $k_c'$ ) for the photoisomers (Scheme III) are not known, but if we assume that  $k_f'$  is the same as that in BR since the photoisomer has a similar absorption spectrum and that  $k_c' = 0$  as the photoisomer is not strained by intramolecular hydrogen bonds, then the rate constant of the rate-limiting step in the PBR → BR isomerization ( $k_p'$ ) is (1–2 ns<sup>-1</sup>)  $5 \times 10^8$  to  $10^9$  s<sup>-1</sup> or approximately 14 times slower than that for BR. The isomerization of PBR back to a Z isomer is only the first step in producing an intramolecular hydrogen-bonded BR.<sup>11</sup> Since the newly regenerated BR (Scheme I) is more open than the BR, it has to rearrange itself to the right conformation to form the BR; this rearrangement process probably occurs in the ground state.

Even though the rate of conversion of Z → E isomers ( $k_p$ ) is much larger than the reverse process ( $k_p'$ ), we are still able to account for the steady-state ratio of concentration,<sup>18</sup> BR/PBR = 5. To do this we use scheme III and calculate the ratio BR/PBR at steady state, assuming for simplicity that the photobilirubin (PBR) is one species. We find that at steady state,

$$[\text{BR}]/[\text{PBR}] = \frac{k_p' \tau_p \left( \frac{k_2}{k_2 + k_2'} \right)}{\left( 1 - (k_c + k_f) \tau_B - \frac{k_2 k_p}{(k_2 + k_2') \tau_B} \right)}$$

where  $\tau_B$  and  $\tau_P$  are the ( $S_1^*$ ) decay times of BR and photoproduct (PBR),  $20 \times 10^{-12}$  and  $10^{-9}$  s, respectively. The other constants are defined in Scheme III, where  $k_c$  and  $k_c'$  represent the internal conversion introduced by twisting the molecule. If we take a "worse case" calculation and assume that all the excited BR or photobilirubin that does not fluoresce goes to isomerization, we obtain the rate constants  $k_p = \tau_B^{-1} = 5 \times 10^{10}$  s<sup>-1</sup>,  $k_p' = \tau_P^{-1} = 10^9$  s<sup>-1</sup>,  $k_c = k_c' = 0$  for a steady state ratio of 5,  $k_2 = 5k_2'$ , although we are unable to determine the magnitude of  $k_2$ . If we include the effects of distortion-induced internal conversion, i.e.,  $k_c \neq 0$ , then at the same steady-state ratio of BR to PBR, we find that  $k_2/k_2'$  decreases. In view of the similarity of the spectral properties of BR and its photoisomers, it seems unlikely that the branching ratio out of intermediate state P can be observed experimentally.

The increase in the decay time of the photoisomer of BR presumably reflects a decrease in the nonradiative rate processes rather than a decrease in  $k_f'$  since the absorption spectra of BR and its isomers are similar. If this is so, then the decrease in the nonradiative rates, particularly  $k_p'$ , is associated with the less strained structure the photoisomers have compared to BR: i.e., these E isomers (Scheme I) have to surmount a larger energy barrier to isomerization than exists in BR excited singlet state.

**Bilirubin Bound to Albumin.** In general terms, the location of BR in HSA and in BSA and its binding sites can be deduced from the fluorescence-lifetime measurements. From the CD and steady-state fluorescence measurements, Lee and Gillespie<sup>29</sup> have shown that BR is bound to HSA in a different way than it is bound to BSA. BR is buried fairly deeply within HSA, while in BSA it is located closer to the surface.<sup>29</sup> The variation of the shorter lifetime ( $\tau_1$ ) representing BR bound to BSA at different pH confirms this hypothesis (Figure 3). As the pH changes from acid to base,  $\tau_2$  changes rapidly, indicating that BR may be more accessible to the aqueous interface and is thus more perturbed by changes of charge or polarity than if it were buried. In HSA, BR is buried deeply,<sup>29</sup> and its decay time ( $\tau_1$ ) remains independent of pH and is also unaffected by chaining the HSA to BR ratio (Figure 4). The longer lifetime ( $\tau_2$ ), which is due to the photoisomers of BR (Z,E, E,Z, and E,E isomers) is very sensitive

(34) West, W.; Carroll, B. H. In "The Theory of the Photographic Process", 3rd ed.; Mees, C. E. K., James, T. H. Eds.; Macmillan Co: New York, 1966; p 243–277.

(35) Hochstrasser, R.; Narva, D. *Photochem. Photobiol.* **1977**, *26*, 595–599.

(36) Hammond, G.; Salties, J.; Lamola, A.; Turro, N.; Bradshaw, J.; Cowan, D.; Counsell, R.; Vogt, V.; Dalton, C. *J. Am. Chem. Soc.* **1964**, *86*, 3197–3217.

to changes in pH, NaCl concentration, and albumin to BR ratio in both BSA and HSA. All these various observations indicate that there are at the minimum two different types of binding sites for the BR and its photoisomers.

We cannot at present speculate about the exact nature of these binding sites, but what appears to be most important is the accessibility of these sites to the aqueous solution. The location of the photoisomers is in a part of the protein at which the isomers can be influenced by external factors such as NaCl concentration or pH. The effect of pH could, for instance, be due to a direct effect on the PBR excited state and/or to change in the protein structure.<sup>1b</sup> We cannot yet distinguish between these two possibilities.

At a HSA/BR ratio of 1 at pH 7.4, increasing the NaCl concentration results in a decrease of the PBR excited-state lifetime (Figure 5,  $\tau_2$ ). As with the effect of pH, the excited molecule and/or the protein<sup>37</sup> could be affected by the presence of ions. The increase in excited-state lifetime of PBR (Figure 6,  $\tau_2$ ) with increasing HSA/BR ratio can be interpreted as the PBR occupying some of many binding sites. Because of their hydrophilicity, these photoisomers will distribute themselves among their available binding sites. As the ratio HSA/BR increases, more binding sites become available and the PBR molecules will then bind more frequently to the most strongly binding sites. This line of reasoning can explain the observation (see Figure 6) of an increase in PBR excited-state decay time with HSA/BR ratio. Under the same conditions, the decay time attributed to BR ( $\tau_1$ ) is unchanged (within experimental error) and is also insensitive (by comparison to PBR) to changes in pH or NaCl concentration (Figures 5 and 6). This insensitivity to environment is consistent with BR being buried in the protein in such a way that it is protected from the solvent. This "hydrophobic" type of binding in the protein is insensitive to charged species at the salt concentrations used in the experiment.<sup>37,38</sup> The hydrophobic nature of some part of HSA is also exhibited by the one tryptophan present, which has a long ( $\sim 6.5$  ns) decay time, comparable to tryptophan in dry proteins such as keratin,<sup>39</sup> and much longer than the decay time ( $\sim 2.5$  ns) in proteins in which the Trp is exposed to the water.<sup>40</sup> The

proximity of BR to Trp has been illustrated by energy-transfer experiments.<sup>3,9</sup>

In bovine serum albumin (BSA), the BR binding sites are known to be near to the surface of the protein, and, consequently, the decay times of BR ( $\tau_1$ ) and the photoisomers ( $\tau_2$ ) are affected by NaCl concentration and BSA/BR ratios. As both components in the fluorescence decay vary under these conditions, we shall not attempt to analyze the effect various binding sites have on the fluorescence decay other than the general effects already described.

### Conclusion

Bilirubin both in solution and bound to albumins has an extremely short decay time in the range 20–70 ps. Concomitant with this fluorescence is that from photobilirubin, which is probably the mixture of the three *E* isomers (*E,Z*, *ZE*, and *E,E*, shown in Scheme I). These photobilirubins emit at a longer wavelength than BR, although the emission spectra overlap considerably. Because of this wavelength difference the circularly polarized fluorescence of BR, which show BR to be in a right-handed helical form in the excited singlet state as well as in the ground state, as observed by CD spectra, can be separated from the circularly polarized fluorescence of the photoisomers. These isomeric compounds have a different excited-state geometry from BR. At pH 4.1 the BR ground state is in the left-handed helical form but changes to a right-handed form in the excited state; this process is fast since it must occur within the excited singlet lifetime, i.e., in less than 70 ps.

The BR readily photoisomerizes at a rate of 1.25 to  $5 \times 10^{10}$  s<sup>-1</sup> in solution and  $1.4 \times 10^{10}$  s<sup>-1</sup> when bound to albumin (HSA), the photoisomerization being the dominant excited-state decay process. The photoisomers can also reconvert back to BR either photochemically at a rate  $\sim 10^9$  to  $5 \times 10^8$  s<sup>-1</sup> or thermally.

When BR is bound to HSA, the binding site is probably protected inside the protein since the BR decay ( $\tau_1$ ) is unaffected by salt concentration or pH. The photoisomers, which are more hydrophilic than BR and consequently lead to a treatment for hyperbilirubinemia, bind to a variety of sites that are exposed on the protein surface as their excited-state decays are sensitive to pH and salt concentration.

**Acknowledgment.** We thank SRC for funding this research and are grateful to Professor Sir George Porter for discussion and encouragement, to Dr. A. F. Drake for his assistance with the CD and CPL, to Professor D. Lightner for samples of pure bilirubin IX $\alpha$  and bilirubin III $\alpha$ , and to Professor R. Bonnett for a sample of half-bilirubin.

(37) Lee, J. J.; Cowger, M. L. *Res. Commun. Chem. Pathol. Pharmacol.* **1972**, *4*, 121–130.

(38) Tanford, C. In "The Hydrophobic Effect"; Wiley-Interscience: New York, 1973; p 9.

(39) Smith, G.; Thorpe, M. R.; Melhuish, W. H.; Beddard, G. S. *Photochem. Photobiol.* **1980**, *32*, 715–718.

(40) Beddard, G. S.; Fleming, G. R.; Porter, G.; Robbins, R. *Philos. Trans. R. Soc. London, Ser. A* **1980**, *A298*, 111–124.